SUPPLEMENTARY MATERIAL

Tree-ring cellulose $\delta^{18}O$ records similar large-scale climate influences as precipitation $\delta^{18}O$ in the Northwest Territories of Canada

FIELD R.D.[1,8*]; ANDREU-HAYLES L.[2,8*]; D'ARRIGO R.D.[2], OELKERS R.[2], LUCKMAN B.H.[3], MORIMOTO D.[3], BOUCHER E.[4], GENNARETTI F.[5], HERMOSO I.[4], LAVERGNE A.[6], LEVESQUE M.[7]

[1]NASA Goddard Institute for Space Studies, Columbia University Dept. Applied Physics and Applied Mathematics, New York, NY, U.S.A.

[2] Tree-Ring Laboratory, Lamont-Doherty Earth Observatory of Columbia University, Palisades, NY, 10964, U.S.A.

[3] Department of Geography, University of Western Ontario, London, Canada.

[4]Department of Geography, GEOTOP, University of Québec at Montréal, Canada.

[5]Institut de Recherche sur les Forêts, UQAT, Amos, Québec, J9T 2L8, Canada.

[6]Carbon Cycle Research Group, Space and Atmospheric Physics, Department of Physics, Imperial College London, London, UK.

[7]Institute of Terrestrial Ecosystems, Department of Environmental Systems Science, ETH Zurich, 8092 Zurich, Switzerland.

[8]These authors contributed equally: Robert D. Field, Laia Andreu-Hayles

*Corresponding authors: robert.field@columbia.edu; lah@ldeo.columbia.edu.

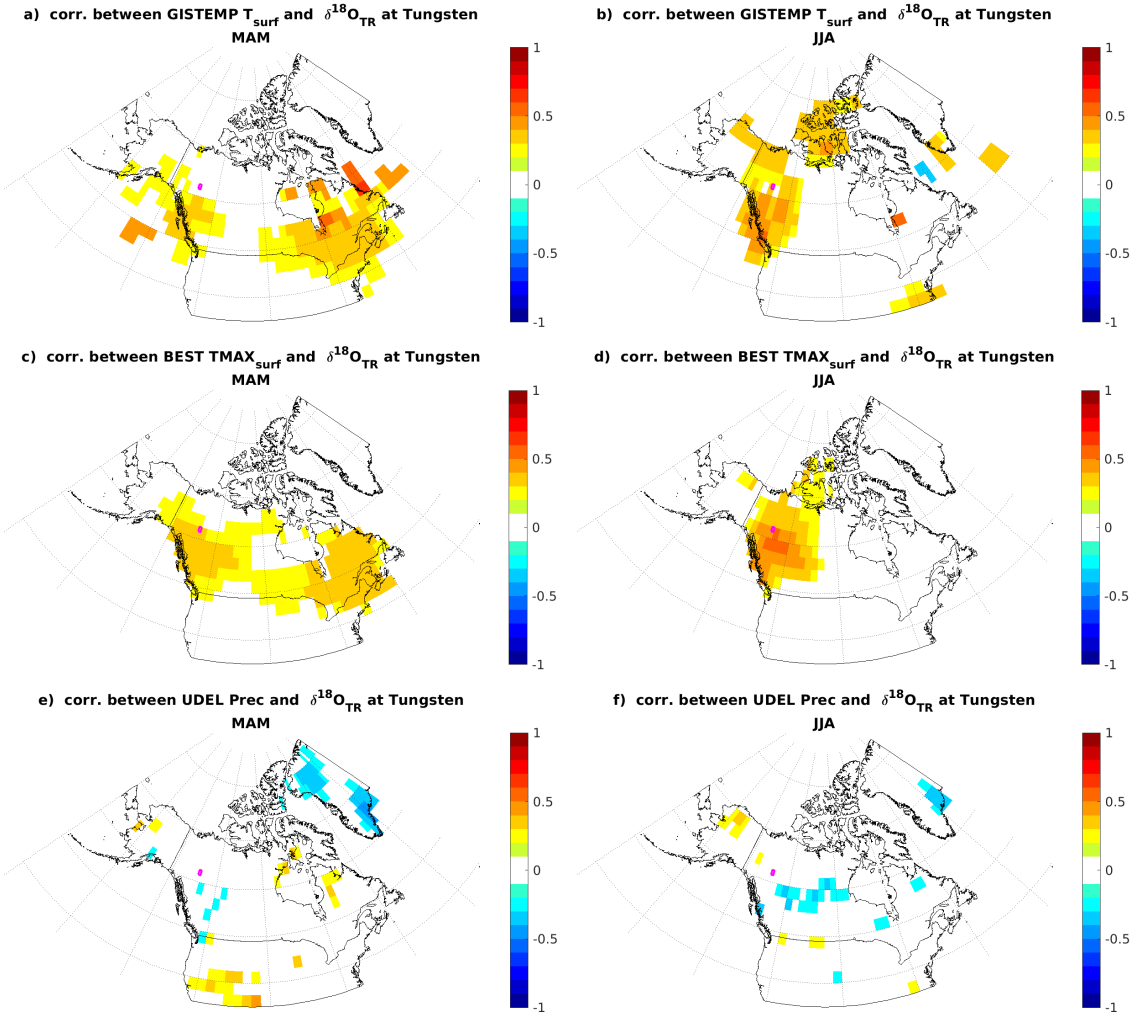

Figure S1. Spatial field correlations between annual tree-ring $\delta^{18}O$ and GISTEMP surface temperature anomaly (top), BEST maximum surface temperature (middle), and University of Delaware (UDEL) precipitation (bottom) over land for spring (March-May, MAM, left) and summer (June-August, JJA, right), over 1938-2002. Correlations with p-values < 0.05 have been excluded. The location of the Tungsten site is shown by the small magenta box.

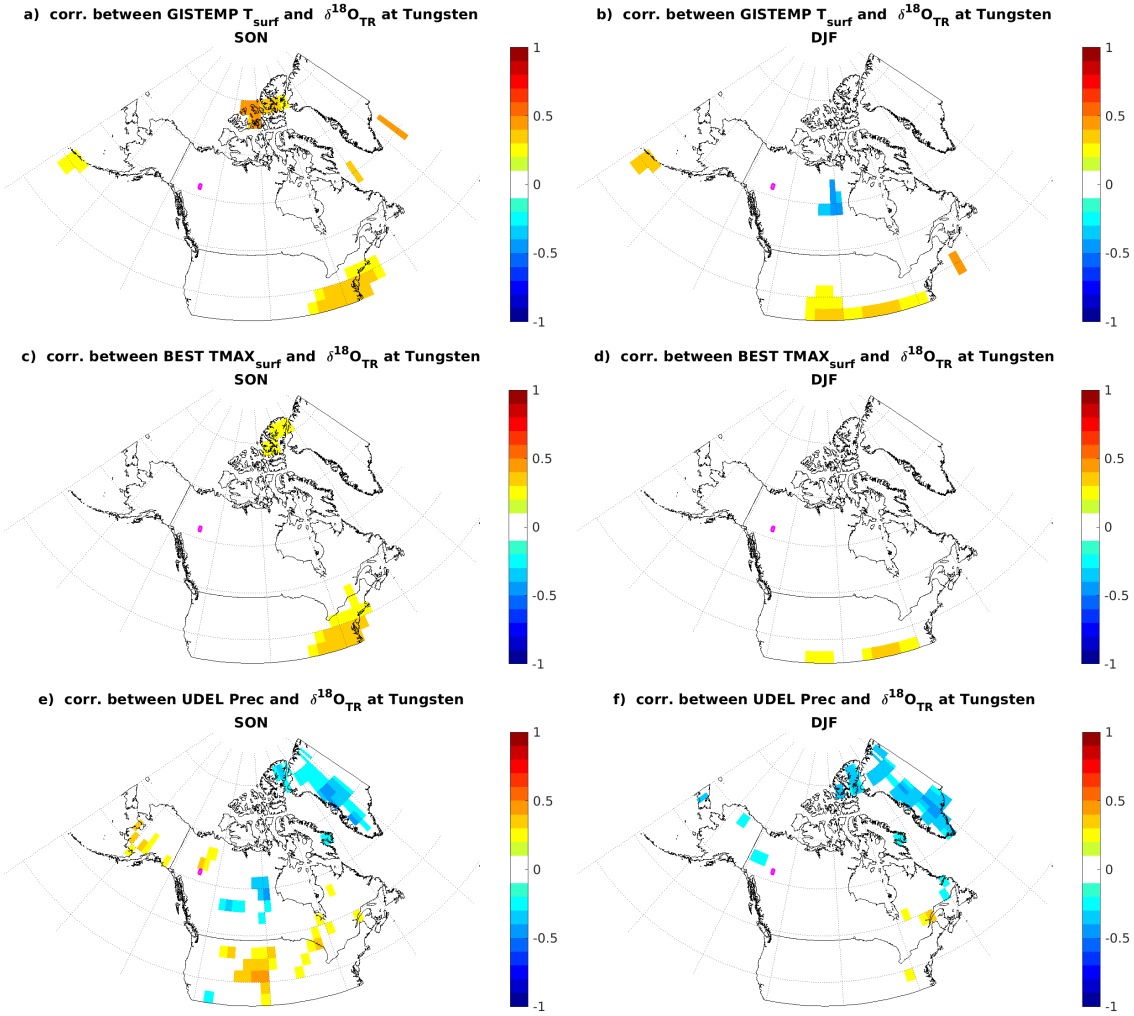

Figure S2. Spatial field correlations between annual tree-ring $\delta^{18}O$ and GISTEMP surface temperature anomaly (top), BEST maximum surface temperature (middle), and University of Delaware (UDEL) precipitation (bottom) over land for autumn (September-November, SON, left) and winter (December-February, DJF, right), over 1938-2002. Correlations with p-values < 0.05 have been excluded. The location of the Tungsten site is shown by the small magenta box.

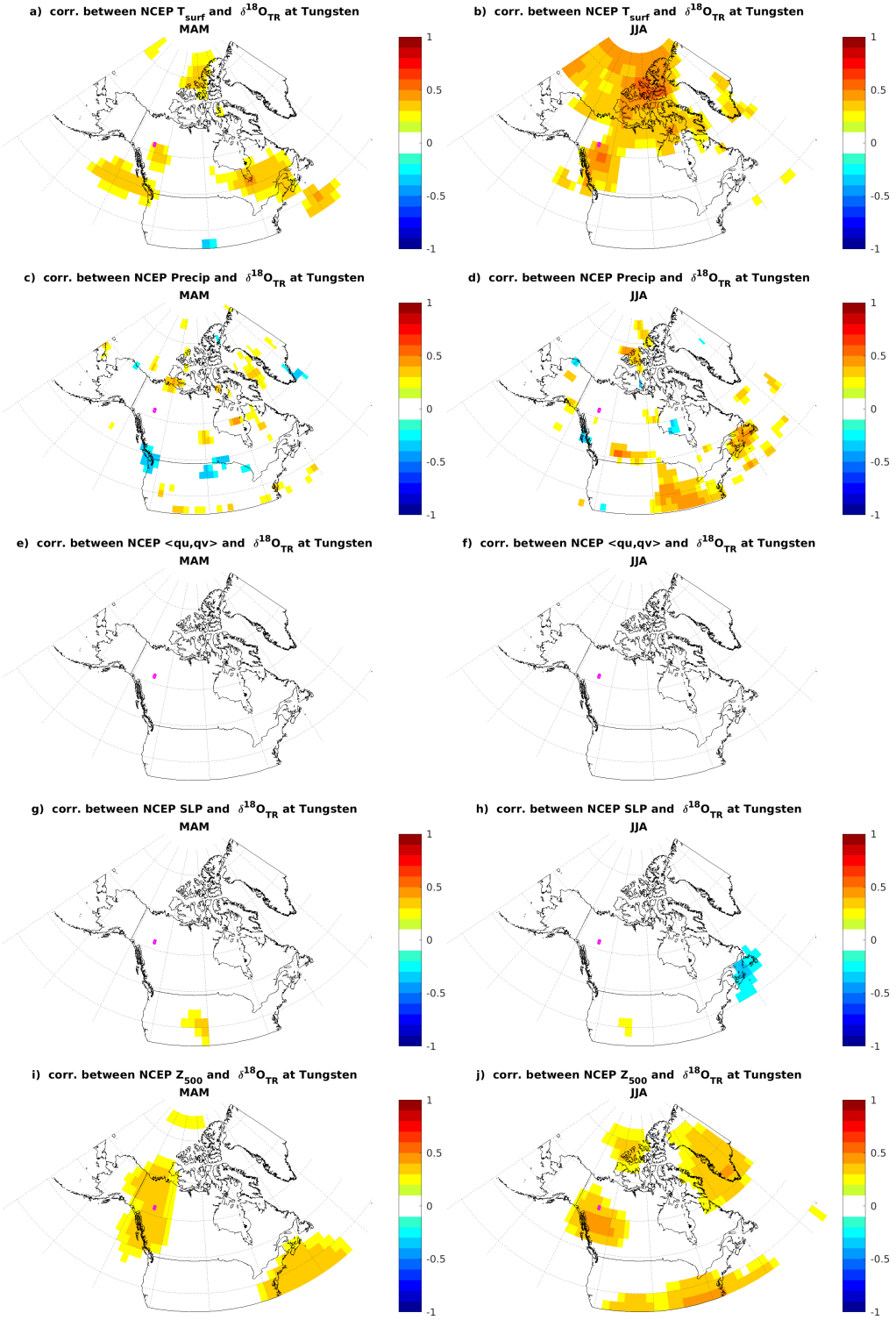

Figure S3. Spatial field correlations between annual tree-ring $\delta^{18}O$ and NCEP surface temperature (T_{surf}), precipitation (Precip), moisture transport at 500 hPa (<qu,qv>), sea-level pressure (SLP), and geopotential height at 500 hPa (Z_{500}) for spring (March-May, MAM, left) and summer (June-August, JJA, right), over 1948-2012. Correlations with p-values < 0.05 have been excluded.

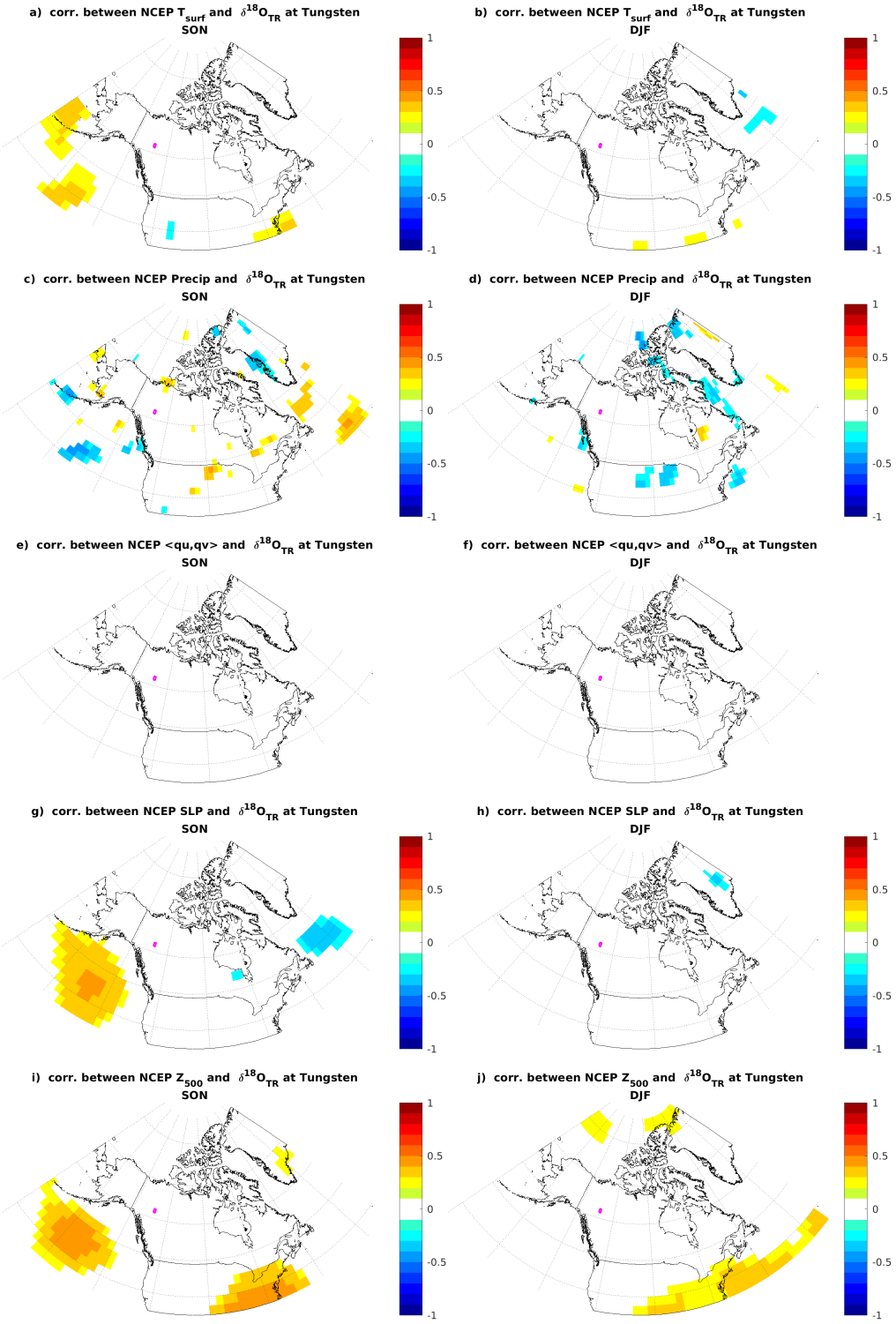

Figure S4. Spatial field correlations between annual tree-ring $\delta^{18}O$ and NCEP surface temperature (T_{surf}), precipitation (Precip), moisture transport at 500 hPa (<qu,qv>), sea-level pressure (SLP), and geopotential height at 500 hPa (Z_{500}) for autumn (September-November, SON, left) and winter (December-February, DJF, right), over 1948-2012. Correlations with p-values < 0.05 have been excluded.

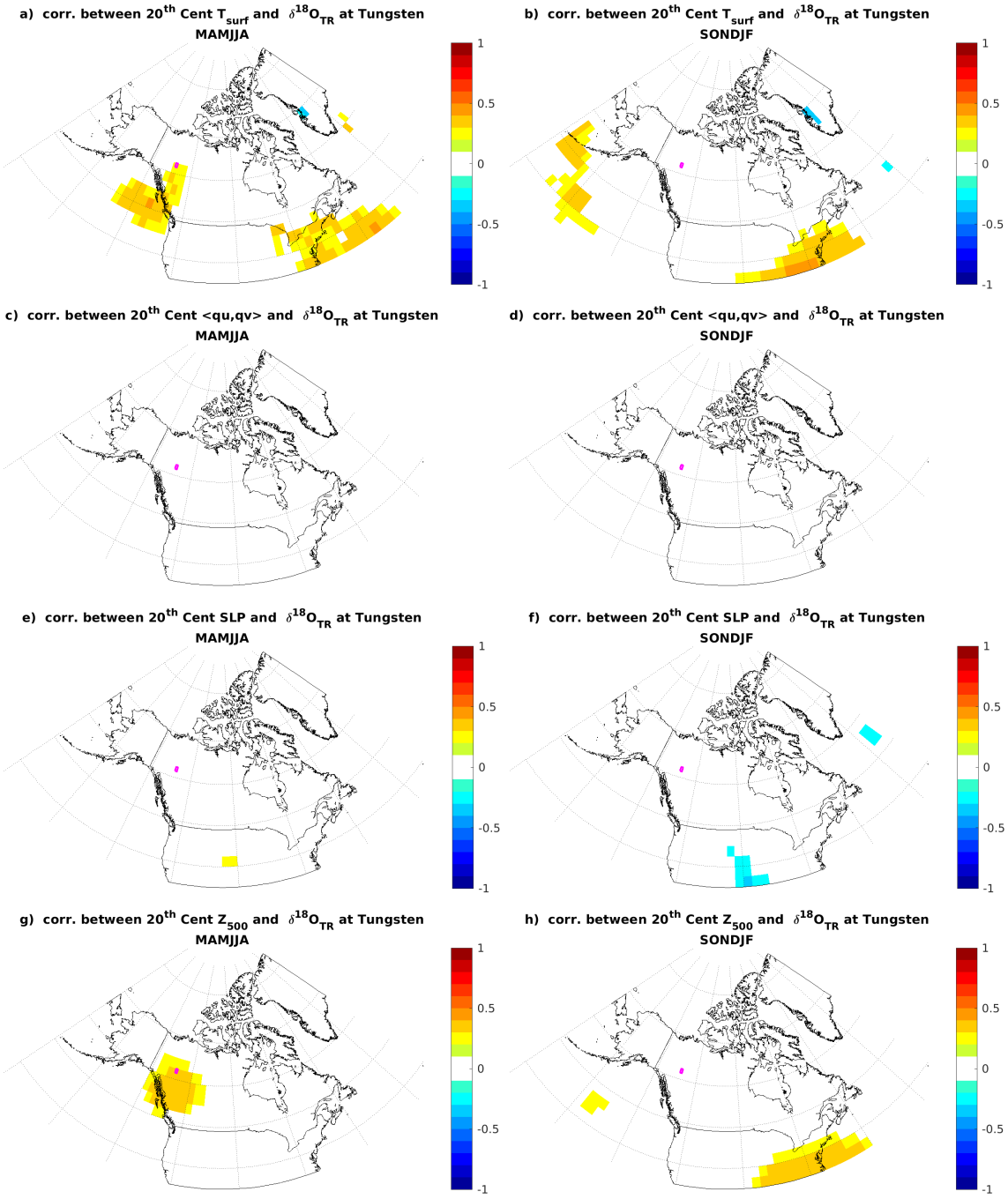

Figure S5. Same as Figure 5 for the period 1948-2002, but replacing NCEP/NCAR reanalysis fields with those from the 20th Century Reanalysis System (Slivinksi et al., 2019).

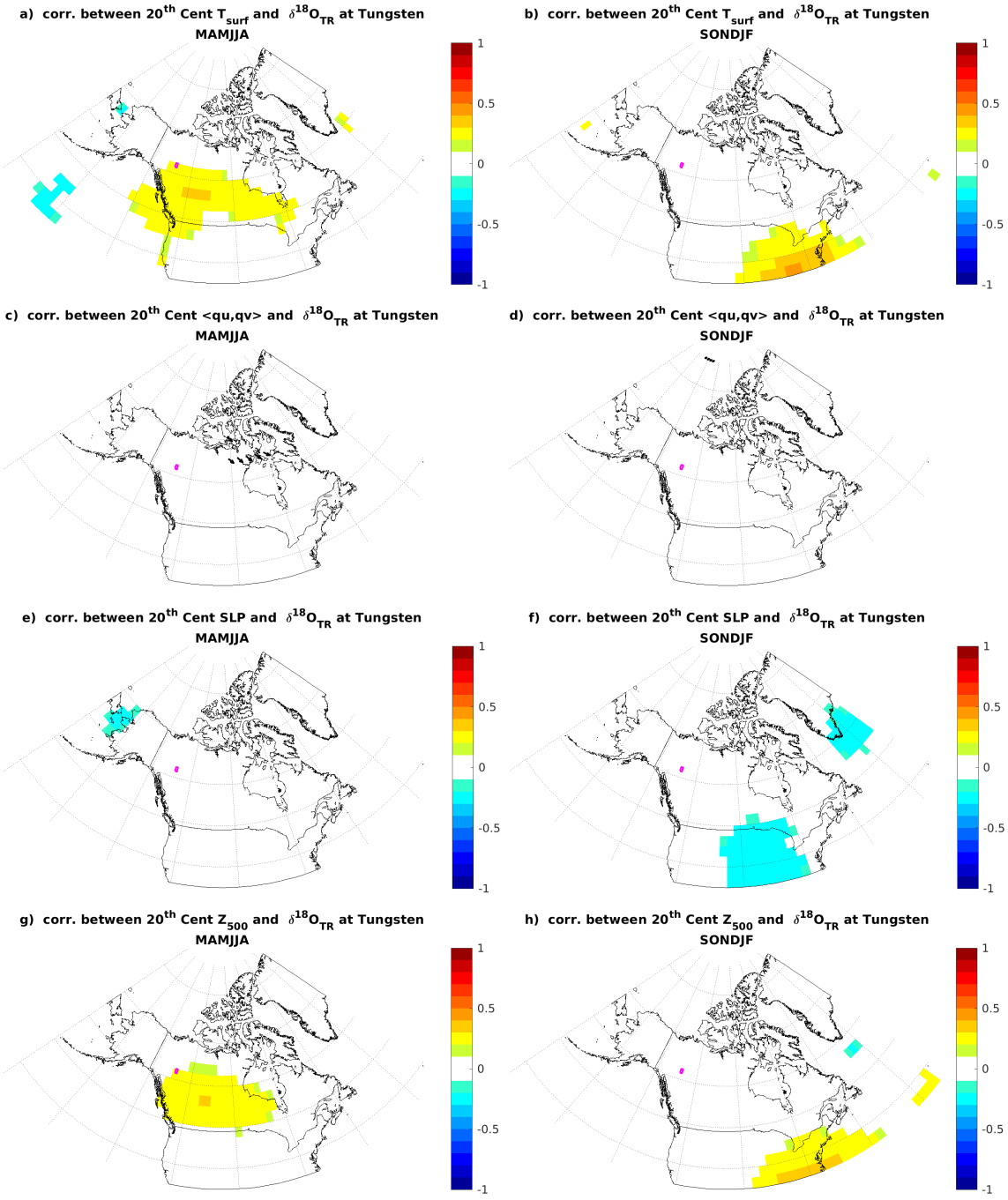

Figure S6. Same as Figure 5, but replacing NCEP/NCAR reanalysis fields with those from the 20th Century Reanalysis System and over the period 1900-2002 (Slivinksi et al., 2019).

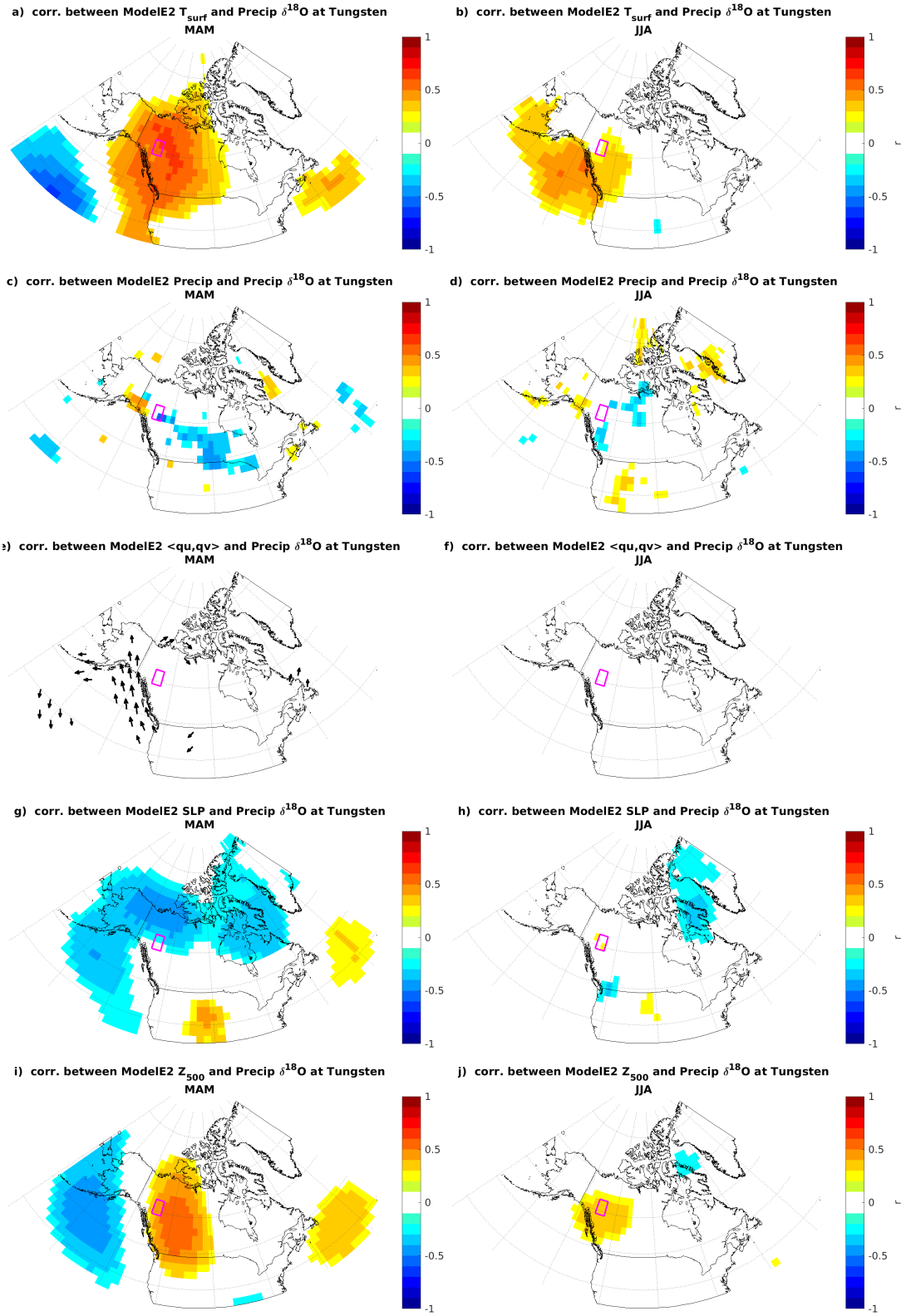

Figure S7. Same as Figure 6, but for spring (March-May, MAM, left) and summer (June-August, JJA, right), over 1948-2012. Correlations with p-values < 0.05 have been excluded.

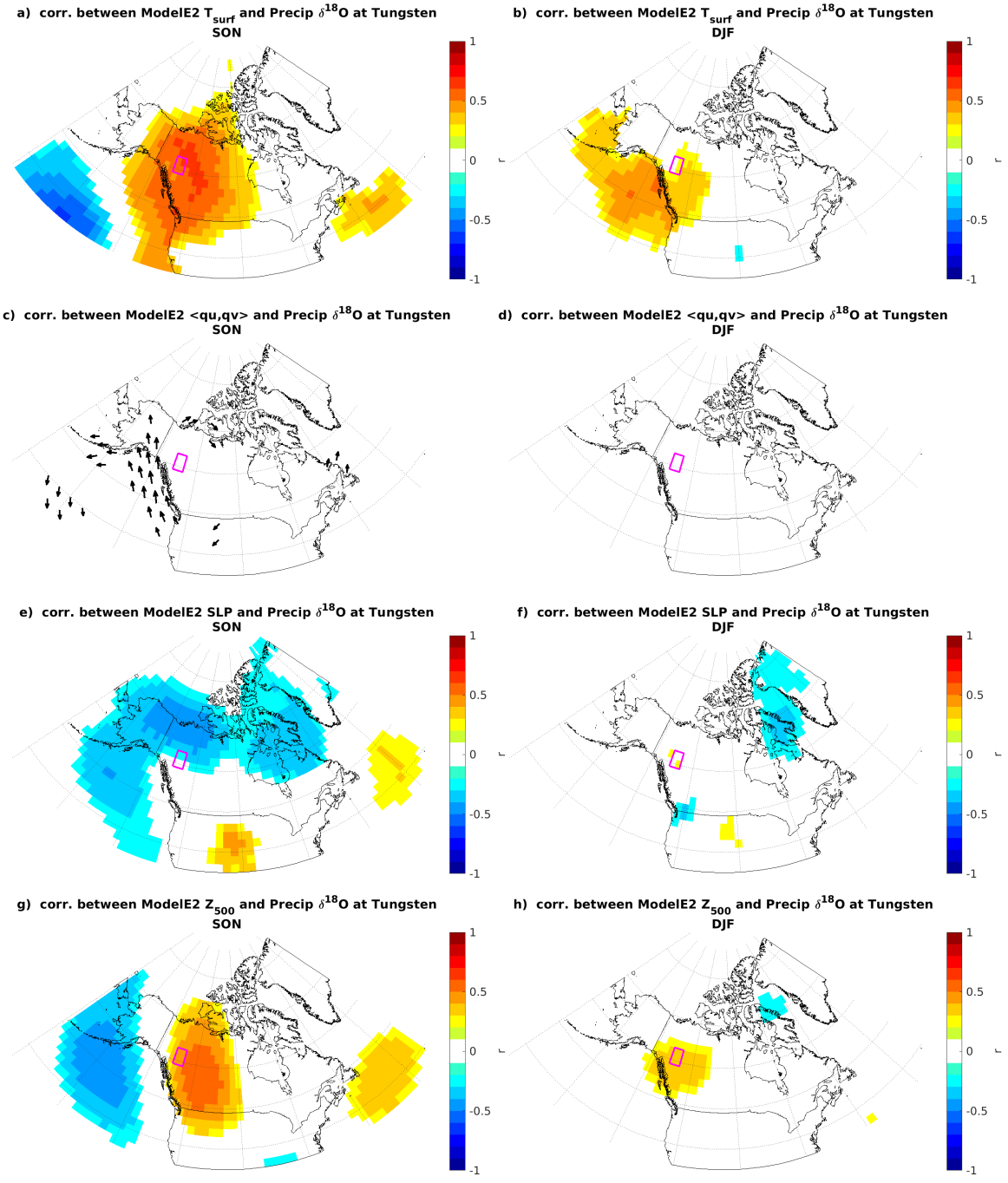

Figure S8. Same as Figure 6, for autumn (September-November, SON, left) and winter (December-February, DJF, right), over 1948-2012. Correlations with p-values < 0.05 have been excluded.